

CFD DISPERSION SIMULATIONS OF COMPRESSED HYDROGEN RELEASES THROUGH TPRD INSIDE SCALED TUNNEL

S.G. Giannisi^{1,*}, A.G.Venetsanos¹, W. Rattigan², K. Lyons²

¹ *Environmental Research Laboratory, National Center for Scientific Research Demokritos, Aghia Paraskevi, Athens, 15341, Greece, sgiannisi@ipta.demokritos.gr*

² *Health and Safety Executive, Harpur Hill, Buxton, SK17 9JN, UK*

ABSTRACT

To achieve the net zero carbon emissions goals by 2050 the transition to cleaner forms and carriers of energy, should be accelerated without though jeopardizing the public safety. Although hydrogen has been deemed to play significant role in the energy transition for years now, there are still concerns for its risks that hamper its widespread implementation in several applications, like for instance automobile applications. Hydrogen-powered vehicles raise concerns about their safety, especially inside confined spaces like tunnels, and thus research on that topic has been intensified during the last years. In this context, experiments have been conducted by UK HSE within the EU-funded project, HyTunnel-CS to examine hydrogen dispersion and deflagration inside a scaled tunnel resulting from fuel cell car, bus and train release.

In this work that was also carried out within the HyTunnel-CS, we present the Computational Fluid Dynamics (CFD) simulations of the HSE unignited experiments. Blowdown tests related to high-pressure hydrogen releases through Thermal Pressure Relief Device (TPRD) installed in car and in train were modeled using the ADREA-HF code. The scope of these simulations was two-fold: a) contribute to the design of the experiments (e.g. indicate sensor positioning, ignition point, etc.) and the interpretation of hydrogen behavior and b) validate the CFD code. For the former, pre-test simulations preceded the experiments to provide design recommendations. When the experiments were conducted the measurements were used for the code validation. Overall, the CFD results are in satisfactory agreement with the experiments. Finally, simulations with different ventilation rates and with model vehicles inside the tunnel were conducted to examine their effect on mixture dispersion and tunnel safety.

Keywords: hydrogen, leak, safety, flammable cloud, explosive concentrations, congestion

1.0 INTRODUCTION

1.1 Motivation for research

The net zero carbon emissions goals for 2050 recognise hydrogen as a key-player for the energy transition. Safety uncertainties can hamper its use beyond industry to other applications, like automobile. Raising public awareness regarding the safety aspects of hydrogen is also important for the growth of hydrogen market. In this context, safety should be ensured across all levels. HyTunnel-CS EU-funded project aimed in studying hydrogen release, dispersion and explosion inside tunnels and other confined spaces, understanding the underlying phenomena and producing recommendations for regulations, standards and codes. The project outcomes addressed existing knowledge gaps for the hydrogen-powered vehicles inside confined spaces, like tunnels and underground parking. Within HyTunnel-CS the current work conducted simulations of high-pressure hydrogen release inside a scaled tunnel based on relevant experiments with the aim to a) validate the CFD code, ADREA-HF, and, to b) investigate a number of factors that could influence hydrogen dispersion inside tunnels.

* Current affiliation: Motor Oil, 12A Irodou Attikou Str.151 24, Maroussi, Greece, sgiannisi@moh.gr

1.2 Short review

Hydrogen safety inside tunnels and other confined spaces is a topic that concerns researchers and stakeholders for quite a long time now, in order to investigate the severity of the consequences and the risks in case of an accident. However, only few research papers dedicated to hydrogen safety inside tunnels are published. Most papers are related to numerical study and less to experimental work. Next, a brief review on experimental studies and CFD studies for hydrogen safety inside tunnels is presented.

Sato et al. [1] and Groethe et al. [2] conducted experiments of hydrogen explosion in reduced-order tunnel. The length of the tunnel was 78.5 m and its cross-section was a part of a 2.4 m diameter circle, i.e. about 1/5 scale of a typical road-tunnel. The experimental results showed that the pressure and impulse were nearly constant over the tunnel length, showing a very significant enhancement of the deflagration when compared with explosions in the free field. They also suggest that ventilation can significantly reduce the hazard caused by deflagration, because of the mixture dilution that results in too lean mixtures to ignite. Kudriakov et al. [3] performed full scale tunnel experiments to investigate the blast wave and fireball resulting from a hydrogen tank rupture. The results showed that not only the mechanical energy of compressed gas but also a fraction of chemical energy contribute to the blast wave strength.

Mukai et al. [6] examined hydrogen dispersion in inclined tunnels using CFD and found that a 2% slope in a long horseshoe-shaped tunnel resulted in hydrogen accumulation near the tunnel ceiling for several dozen minutes, whereas in underwater tunnels with a trough slope, hydrogen was rapidly cleared from the tunnel. Venetsanos et al. [7] conducted CFD simulations with hydrogen release from a bus inside a horse-shoe shaped tunnel to examine both dispersion and combustion. In dispersion simulations hydrogen is accumulated at the tunnel ceiling and forms a considerable flammable volume depending on the release conditions. The combustion results showed a maximum overpressure of 150 kPa for the worst case scenario, i.e. release at 35MPa simultaneously from all PRDs.

Another CFD study in tunnels was that of Middha and Hansen [8], who investigated releases from hydrogen cars (containing 70 MPa gas tanks releasing either upwards or downwards or liquid hydrogen tanks releasing only upwards) and buses (containing 35 MPa gas tanks releasing upwards) for two different tunnel layouts and several ventilation rates. The worst-case involved the tunnel filling with stoichiometric hydrogen gas clouds of varying size resulting in very high overpressures (the highest predicted pressure was almost 1200 kPa for a 1000 m³ gas cloud). However, this scenario assumes that the full gas inventory is being mixed homogeneously at stoichiometry, an unrealistic scenario.

Kumar et al. [7] showed that the increased ceiling height associated with arched cross-section tunnels reduces the hazard associated with the release of hydrogen, due to increased dilution of the mixture and a reduction in the momentum of the impinging jet. However, it was noted that the presence of obstacles, e.g. light armatures or fans, could add some turbulence to flame propagation and make explosions more severe. Momferatos et al. [8], Toliás et al. [9], Molkov et al. [12] and Baraldi et al. [13] have simulated combustion experiments [14] using the CFD methodology. Based on these works, it was shown that CFD is capable of simulating hydrogen combustion inside tunnels and predicting the generated overpressures satisfactorily.

Other CFD studies related to hydrogen dispersion and combustion modeling inside tunnels are that of Houf et al. [15] and of Bie and Hao [16]. Houf et al. [15] examined the case of a release from 700 bar through the TPRD in a fuel cell car inside a transversely ventilated tunnel. They investigated the distribution of the ignitable cloud and tested several ignition locations and ignition delays to predict the generated overpressures and impulses. Based on the CFD results the worst case (~3 barg) was ignition above the vehicles 10 cm from the tunnel ceiling with 5 s delay. Bie and Hao [16] performed simulations of hydrogen dispersion and combustion in subsea tunnel. The results revealed that

ventilation influences greatly the distribution of hydrogen and reduces the generated overpressures at the points downwind the release.

More recently, Hansen et al. [17] conducted a CFD study to assess to what extent higher TPRD release rates than typically used for FCVs may be applied without compromising safety. The main conclusions from that study was that in heavy duty vehicles TPRDs should be directed upwards to limit the size of reactive clouds and the associated risk to people, and that the TPRDs should be designed such to result in a release rate below 200 g/s.

Within the HyTunnel-CS project two different experimental series by CEA and HSE have been performed [4], [5] to investigate hydrogen behaviour inside tunnels. CEA conducted experiments inside a real tunnel using helium as hydrogen surrogate. The releases occurred downward or upward to simulate the opening of a TPRD with or without the rollover of the damaged car. The main conclusions of this experimental work were that a) tilting the TPRD 45° backwards will prevent the formation of an explosive atmosphere under the vehicle, b) using smaller TPRD sizes (1 mm diameter) greatly restricts the extension of the flammable cloud from the bottom to the top of the tunnel but results in a greater persistence of this explosive atmosphere, c) natural ventilation (<1 m/s) does not affect the maximum concentration but drives the transport and dilution of the cloud after the release is complete, d) the presence of geometric changes in the shape of the tunnel at the top or a highly variable roughness can modify the dispersion, creating areas of accumulation that are more slowly diluted. HSE conducted unignited and ignited experiments inside a scaled tunnel. They examined different scenarios, releases from car, bus and train, with and without congestion with mechanical and natural ventilation. The general conclusions were for the car scenario even with the low ventilation speed the mixture was well diluted with most peak concentrations below 4 %. For the bus and train scenarios, large flammable cloud was formed that reached the exit of the tunnel. High wind speeds increased the speed of progression of the hydrogen cloud, reducing potential hazard exposure and also slightly increased the mixture dilution. More detailed discussion about these experiments follows in this paper, as they are the ones simulated.

Finally, LaFleur et al. [18] and Ehrhart et al [19] performed a thorough risk assessment investigating a number of possible scenarios involving a hydrogen vehicle crash inside a tunnel. Based on the risk analysis it was shown that there will be no additional hazard from the hydrogen fuel and that if the hydrogen does ignite, the most likely consequence will be a jet flame resulting from the pressure relief device due to a hydrocarbon fire (0.03–1.8% probability).

1.3 Current work

In the present work the recent HSE scaled tunnel experiments with unignited release are simulated using the ADREA-HF CFD code. Initially, various pre-test simulations were performed to assess the hydrogen distribution inside the tunnel and provide useful information to the experimentalist before the launch of the experiments, i.e. sensor positioning, ignition position and delay, etc. After the completion of the experiments validation simulations were carried out to evaluate the performance of the CFD code to accurately reproduce the associated physical phenomena. For the validation two scenarios were selected: release from a car and release from a train. In this paper, only the validation simulations are shown. Additional sensitivity simulations were performed to evaluate the ventilation efficiency and the congestion effect on hydrogen dispersion inside tunnels.

2.0 DESCRIPTION OF EXPERIMENTS

HSE Science and Research Centre conducted a series of experiments investigating the release, dispersion and combustion properties of pressurised gaseous hydrogen in a tunnel. The main objective of this experimental series was to produce hydrogen dispersion and combustion data for realistic (scaled) hydrogen releases in a tunnel. The releases would simulate a thermally activated pressure relief device (TPRD) in operation on hydrogen vehicles. The data generated can be used to validate

numerical models, which can then be used to predict the total flammable extent for realistic accident and release scenarios.

A scaled tunnel was used and all relevant parameters (like diameter, inventory, storage pressure) were scaled accordingly, so as the measured concentration distribution to be similar of that in a real scale tunnel. The tunnel has a nominal diameter of 3.7 m and total length of 70 m. Inside the tunnel there was a concrete base with a 0.45 m depth, which supports a set of rails and the release structure.

Four scenarios were tested: Car, Bus, Train 1, and Train 2. Each scenario had different inventory, nozzle size, and storage pressure. Table 1 provides the scaled conditions for each case. It should be noted that the actual (non-scaled) pressure considered for the car, bus and train was 700, 350 and 350 barg, respectively. For more details about the experimental facility, instrumentation and conditions refer to [5].

Table 1. The scaled conditions for the different experimental scenarios.

	Total Inventory (kg)	Pressure (barg)	Tank Volume (litres)	Diameter
CAR	0.46	118	53	2.2
BUS	3.40	310	159	4.0
TRAIN 1	5.07	510	159	5.7
TRAIN 2	5.54	580	159	4.7

The release was at the center of the tunnel along its length and slightly offset its centerline located at $y=0.61$ m. The height of the release depends on the scenario. For the car case the release was assumed under the vehicle at around 0.136 m above the tunnel floor with downwards direction, while for the train the release was assumed from the top of the train at around 1.54 m above the tunnel floor with upwards direction.

For the ventilation a set of seven fans were installed at the end of the tunnel to provide a semi-consistent wind speed. Aluminium honeycomb flow straighteners were also used to reduce the ‘swirl’ induced by the large axial fans. Two different wind speeds were tested: 1.25 m/s and 2.4 m/s.

Tests with model vehicles inside the tunnel were also performed to investigate the effect of congestion on the dispersion and the generated overpressure in case of ignition. However, due to damage of the fans after the first ignition test there are no experimental data available for unignited releases with forced ventilation (only with natural ventilation for the bus and the train 2 scenario). The vehicles were placed 4 m downwind the release in both lanes. The vehicles layout for the car and the train scenario is shown in Figure 7.

To generate valuable data, both source term and dispersion measurements were required. Pressure and temperature inside the tank and at the nozzle manifold were measured. Mass flow rate was not measured directly and was calculated based on the other measured parameters. A set of 16 hydrogen sensors were deployed to measure the concentration across the tunnel, each with an independent sampling line and pump. Each sensor has its own delay time depending on its position, which is available in the experimental data [5]. Sensor position is given in Table 2.

3.0 DESCRIPTION OF SIMULATIONS

3.1 Modeling strategy and governing equations

For the simulations the ADREA-HF CFD code was used, which solves the 3D time-dependent conservation equations of mass and momentum. The conservation equation of hydrogen mass fraction is also solved and the $k-\epsilon$ turbulence model was used. The conditions were assumed isothermal, as the hydrogen was assumed to be released at ambient temperature following the Birch 84 notional nozzle approach [20], which was employed to model the under-expanded jet that is formed downstream the nozzle. This approach assumes that the jet expands to ambient pressure downstream the nozzle having sonic velocity and ambient temperature. With known variables the mass flow rate, the pressure and the

temperature, hence the density, and the velocity we calculated the notional area. These conditions were set as hydrogen inlet boundary conditions in the dispersion simulation. The transient source of the blowdown release was modelled by applying forcing function with transient source area based on the transient mass flow rate computed from experimental data (tank pressure and temperature). The velocity at the source was constant and equal to sonic until the end of the release.

The mathematical equations that were solved are:

$$\frac{\partial \rho}{\partial t} + \frac{\partial \rho u_i}{\partial x_i} = 0 \quad (1)$$

$$\frac{\partial \rho u_i}{\partial t} + \frac{\partial \rho u_i u_j}{\partial x_j} = -\frac{\partial P}{\partial x_i} + \frac{\partial}{\partial x_j} \left[(\mu + \mu_t) \left(\frac{\partial u_i}{\partial x_j} + \frac{\partial u_j}{\partial x_i} \right) \right] + \rho g_i \quad (2)$$

$$\frac{\partial \rho q_{H_2}}{\partial t} + \frac{\partial \rho u_j q_{H_2}}{\partial x_j} = \frac{\partial}{\partial x_j} \left[\left(\rho D_{H_2} + \frac{\mu_t}{Sc_t} \right) \frac{\partial q_{H_2}}{\partial x_j} \right] \quad (3)$$

where ρ - mixture density, kg/m³; u - velocity, m/s; P - pressure, Pa; g - gravitational acceleration, m/s²; μ , μ_t - laminar and turbulent viscosity respectively, kg/m/s; Sc_t - turbulent Schmidt number, dimensionless; D - molecular diffusivity, m²/s; q - mass fraction. The subscripts i and j denote the Cartesian x , y and z coordinates. The turbulent Schmidt number was set equal to 0.72. Ideal gas was assumed.

A steady state simulation without release was first solved to obtain the ventilation profile. In this simulation the ventilation velocity was imposed uniformly along the tunnel opening. The established steady state velocity field is set as initial and inflow boundary condition in the CFD dispersion simulation. Approximate values for k and ϵ across the ventilation boundary were imposed.

3.2 Numerical details

The system of the partial differential equations was solved numerically. For the space discretization the high order scheme, MUSCL, was used in all variables, while for the time integration the 1st order upwind scheme was employed. Wall boundary conditions were applied to all solid surfaces (tunnel walls, ceiling, ground, vehicles). At all open boundaries the constant pressure boundary condition was imposed and for the hydrogen concentration the given value, if inflow and zero gradient if outflow condition was applied. At the ventilation opening given value boundary condition was applied based on the 3D simulation without release (see Section Modeling strategy and governing equations).

3.3 Computational domain and grid

The grid was Cartesian and the porosity method was used to account for block (flow domain) and non-blocked (solid) cells. At the one opening of the tunnel with the ventilation no domain extension was considered. At the other opening (the open exit) the domain was extended in all directions to avoid imposing boundary conditions exactly at the opening, which can lead to inaccurate results [21]. However, around and above the tunnel solid boxes were placed to reduce the number of active cells and consequently the run time of the simulations without affecting the results. The initial source area was discretized by 4 cells. As release progresses the source is decreased and at some point the cells are larger than the source area. However, the largest mass of the inventory is already released by that time and the numerical errors are not expected to be large.

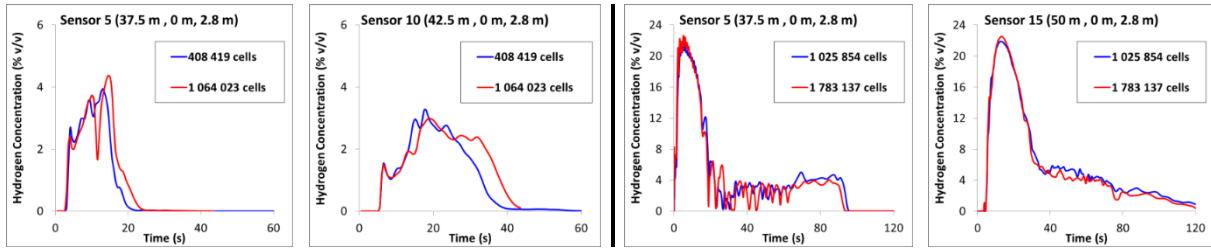


Figure 1. Grid sensitivity study for the car (left) and the train 2 (right) at two sensors. The coordinates of the sensors are in respect to the ventilation opening and the tunnel floor. The release point is located at ($x=35$ m, $y=-0.61$ m).

Denser grids were tested by using a smaller expansion ratio close to the release along all directions. For the car scenario the examined grid had size 408 419 and 1 064 023 cells. For the train scenario the different grids consisted of 1 025 854 and 1 783 137 cells. The grid sensitivity study of the car scenario (Figure 1, left) showed that the results of both grids were very similar. For the comparison with the experiment the fine grid was used, while for the sensitivity study the coarse grid was used. For the train scenario the grid had little impact on the results in most of the sensors. Thus, the coarse grid was considered independent and was used throughout this study.

4.0 RESULTS AND DISCUSSION

Pre-test simulations were performed before the experiments were conducted and provided useful information for the sensor's positioning, the ignition position and ignition delay. The results can be found in [4]. In this paper, we focus on the validation and sensitivity simulations.

4.1 Validation simulations

For the validation the car and train 2 scenarios were selected. Figure 2 shows the comparison between simulations and experiments for the car scenario and Table 2 shows the maximum predicted and experimental concentration at all sensors and their relative error. According to Table 2 the maximum concentration is under predicted at most of the sensors for the car scenario.

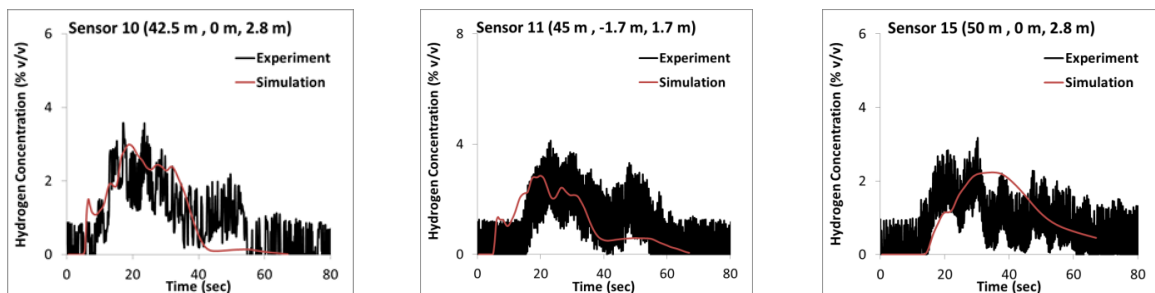


Figure 2. Comparison of the time series of hydrogen concentration at several sensors for the car scenario. The coordinates of the sensors are in respect to the ventilation opening and the tunnel floor with the release point located at (35 m, -0.61 m, 2 m).

To better understand the dispersion dynamics and the cloud behavior the flammable mixture (iso-surface of 4 % v/v H_2) at several times during the blowdown release was produced and illustrated in Figure 3. The jet, which was released vertically downwards, hits the tunnel floor and starts to spread. It ascends along the tunnel walls due to the positive buoyancy creating a bifurcation (ring-like structure). Ventilation air drifts the mixture downwards the release for few meters (flammable concentrations were extended approximately 6 m from the release point). The flammable cloud does not fill the entire cross-section of the tunnel and as time progresses and release rate decreases it is limited to a region close to the release and the tunnel floor (below the hypothetical vehicle from where the release took place).

Table 2. Comparison of the maximum concentrations at all sensors for the car and the train scenario.

	Car scenario			Train scenario		
	Simulation Max (% H2)	Experiment Max (% H2)	Relative error	Simulation Max (% H2)	Experiment Max (% H2)	Relative error
Sensor 2 (34, 0.0, 2.8 m)	3.7	1.1	240.40%	13.7	17.3	-20.52%
Sensor 3 (37.5, 0.0, 0.5 m)	3.7	6.9	-46.07%	18.0	37.5	-52.11%
Sensor 4 (37.5, 0.0, 1.7 m)	4.2	3.4	22.81%	18.7	19.7	-4.87%
Sensor 5 (37.5, 0.0, 2.8 m)	4.4	5.0	-12.55%	21.9	22.4	-2.32%
Sensor 6 (40, -1.7, 1.7 m)	3.6	3.8	-5.21%	24.9	23.0	8.21%
Sensor 26 (40, -1.2, 1.7 m)	2.0	3.7	-46.03%	22.8	21.9	4.05%
Sensor 8 (42.5, 0.0, 0.5 m)	3.2	2.8	13.93%	22.3	21.9	1.89%
Sensor 9 (42.5, 0.0, 1.7 m)	3.0	2.8	8.11%	21.7	21.4	1.28%
Sensor 10 (42.5, 0.0, 2.8 m)	3.0	3.6	-16.90%	21.6	21.4	0.79%
Sensor 11 (45, -1.7, 1.7 m)	2.9	4.1	-30.45%	22.8	22.0	3.71%
Sensor 12 (45.0, -1.2, 1.7 m)	2.1	3.7	-43.52%	22.0	21.5	2.51%
Sensor 13 (50.0, 0.0, 1.0 m)	2.3	2.7	-13.51%	21.8	21.0	3.95%
Sensor 14 (50.0, 0.0, 1.7 m)	2.5	3.8	-35.00%	21.8	20.6	5.96%
Sensor 15 (50.0, 0.0, 2.8 m)	2.2	3.2	-30.23%	21.9	21.3	2.78%
Sensor 16 (60.0, 0.0, 2.8 m)	3.9	3.0	28.93%	21.5	20.8	3.60%

This behavior along with the maximum concentration observed in the experiment and predicted by the simulation indicates that in case of a release from a car TPRD inside a ventilated tunnel the hazardous area is limited to a region close to the leak, i.e. underneath the car and on the top above the car (along the ceiling). However, the concentration on the top falls below the flammable limit in about 40 seconds from the start of the release. Based on all the above, the car scenario can be considered as a not very dangerous scenario.





Figure 3. Predicted 4 % v/v H₂ iso-surface at 1, 6, 10, 20, 30 and 40 sec for the car scenario.

Figure 4 shows the experimental and predicted time series for the train scenario at several sensors. There is one sensor upwind the release (sensor 2), while the rest sensors are downwind the release at different distances and different heights. The agreement of the simulation with the experiment is very good for most of the sensors. Higher discrepancies are observed at the two sensors closer to the release (sensor 2 and 3). This is also supported Table 2. Based on the relative error the maximum concentration is predicted with high accuracy at most of the sensors (less than 5% relative error) with a slight tendency to over predict the peak concentration. The largest differences are observed at the sensors 2 and 3, where the concentration is under predicted. Sensor 2 (-20.5% error) is upwind the release and close to the ceiling, while the sensor 3 (-52% error) is downwind the release at 0.5 m height. However, sensor 3 measured concentration levels higher than all the other sensors even the sensors at the same location but greater heights. This behavior seems unphysical and was attributed to sensor failure [22].

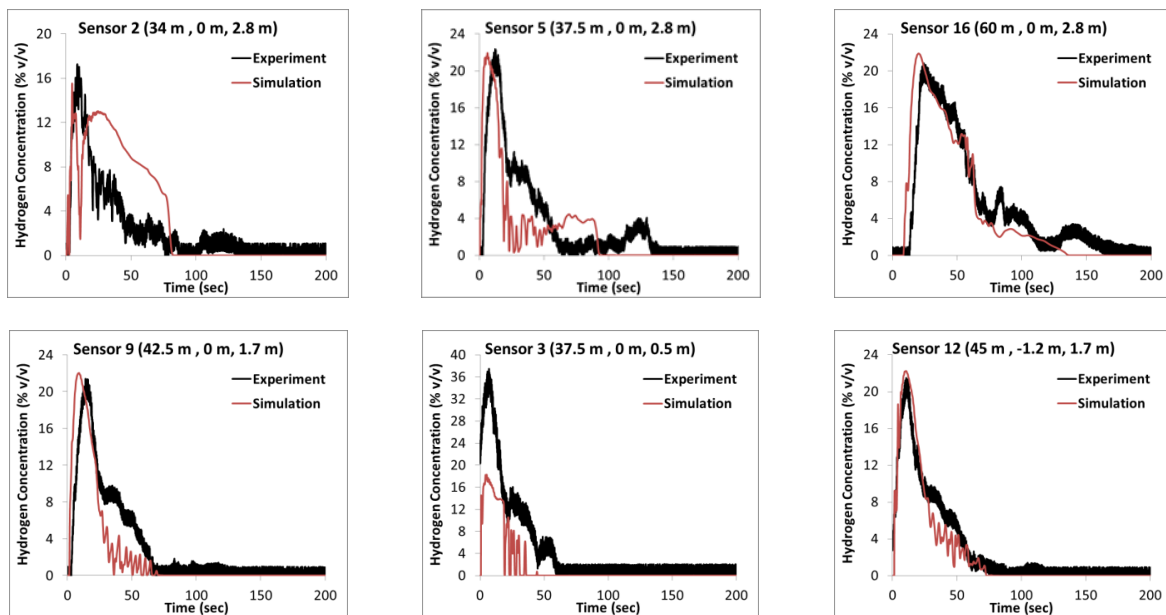


Figure 4. Comparison of the time series of hydrogen concentration at several sensors for the train scenario. The coordinates of the sensors are in respect to the ventilation opening and the tunnel floor with the release point located at (35 m, -0.61 m, 2 m).

Based on both the experiment and the simulation the mixture spreads downwind the tunnel almost undiluted, as the peak concentration is very similar and equal to around 21% v/v at all sensors. The upwind spread of the mixture (towards the ventilation opening) is limited because of the ventilation and thus the peak concentration at the only upwind sensor (sensor 2) is lower (< 20 % v/v) than the downwind sensors. The flammable cloud exits the tunnel through the downwind opening (the one without the ventilation) at around 10-20 sec and rises up due to buoyancy, as shown in Figure 5.

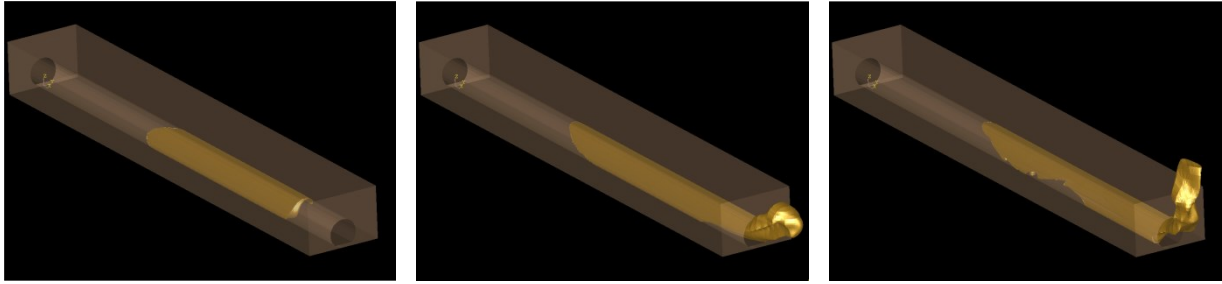


Figure 5. Predicted 4 % v/v H₂ iso-surface at 10, 20 and 40 sec for the train scenario.

4.2 Sensitivity studies

Simulation with higher ventilation rate (2.4 m/s) was performed for the train scenario. The comparison between the simulations with the two ventilation rates along with the experimental data is presented in Figure 6. Comparing the simulation with ventilation rate 2.4 m/s with the respective experiment an over prediction is observed contrast to the case with 1.25 m/s rate where the results were in very good agreement with the experiment (see Validation simulations). Higher variations in the ventilation rate in the case with the higher rate can be a possible reason for the lesser agreement of the simulation with the experiment. Note that in the simulations the ventilation rate was constant in time, while in the experiment there were fluctuations.

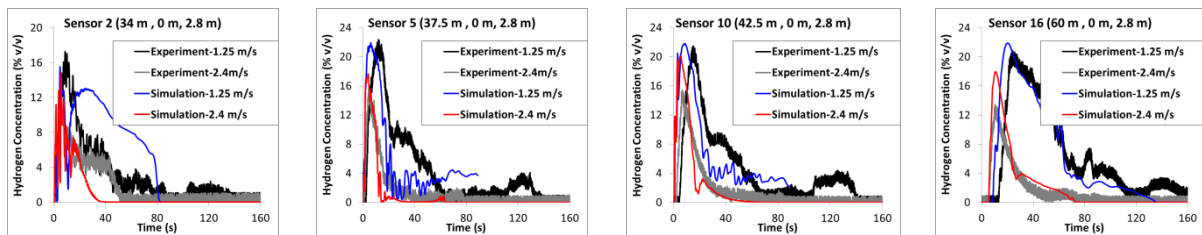


Figure 6. Comparison of the concentration time series at several top sensors for the two ventilation rates.

Table 3 gives a comparison of several safety parameters for the two ventilation rates based on the simulation results. The flammable volume increases with increasing ventilation rate, but the volume at near stoichiometric concentration (25-35% v/v) is reduced. With higher ventilation rates the mixture is spread more downwind resulting in larger flammable volumes, but it is also more diluted (lower concentrations within the flammable cloud), as it is indicated by the reduced volume of the mixture at near stoichiometric concentration. Finally, the flammable mixture inside the tunnel remains for considerable lower time in the case with the high ventilation rate (almost half time).

Table 3. Safety parameters for the different sensitivity cases.

	Maximum Flammable volume (m ³)	Maximum volume with 25-35 % concentration range (m ³)	Maximum concentration (over all the deployed sensors)	LFL downwind distance from the release (m) [†]	8% v/v downwind distance (m) [‡]	Residence time of flammable cloud inside the tunnel (sec) [§]
Ventilation rate 1.25 m/s – no vehicles	498	7.3	24.8 %	46.36	42.4	110
Ventilation rate 2.4 m/s – no vehicles	633	2.9	21.7 %	47.17	43.7	65
Ventilation rate 1.25	448	7.0	24.9 %	47.6	42.5	110

[†] The flammable cloud was extended outside the tunnel.

[‡] Hydrogen at concentration below 8% has a very low reactivity and it is challenging to ignite.

[§] This is an approximate value.

m/s – vehicles						
----------------	--	--	--	--	--	--

It should be noted that a simulation with higher ventilation rate (3.4 m/s) was also tested leading to even lower peak concentrations, but still above 4% v/v. In the future, it would be interesting to conduct a study to explore if there is a ventilation rate of practical value that could considerably limit the formation of flammable cloud inside the tunnel or if there is an upper threshold above which the ventilation has no additional effect.

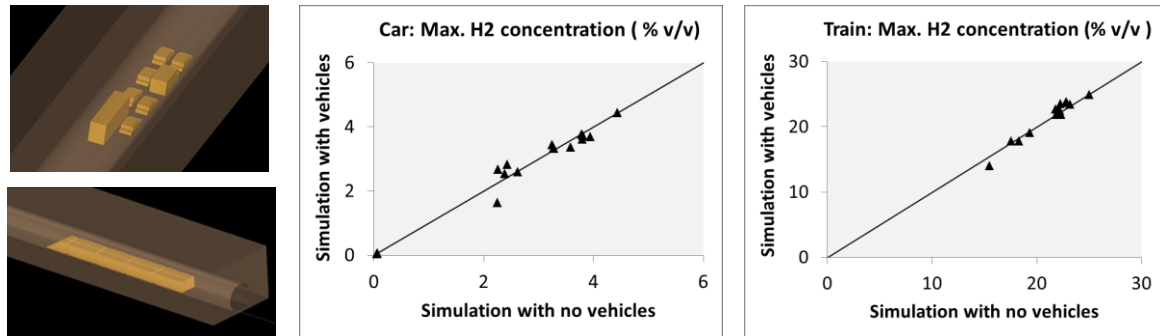


Figure 7. The vehicles layout for the car scenario (left, top) and the train scenario (left, bottom), and the maximum concentration for the simulation with no vehicles versus the simulation with vehicles for the car scenario (center) and the train scenario (right).

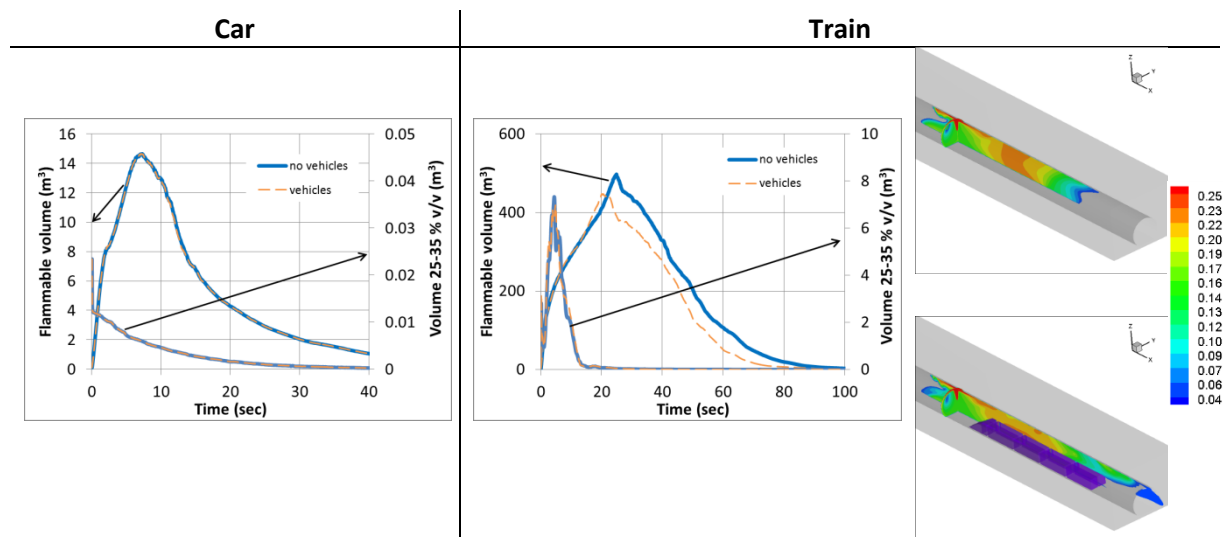


Figure 8. Flammable volume and volume with concentrations ranged between 25-35 % v/v for the simulation with no vehicles versus the simulation with vehicles for the car scenario (left) and the train scenario (right). Contour plot along the release x-plane ($x=35$ m) and y-plane ($y=0.61$ m) at 10 sec for the case without vehicles (right, top) and the case with vehicles (right, bottom) for the train scenario.

An additional simulation with vehicles inside the tunnel was performed for both scenarios (car and train with 1.25 m/s ventilation rate) to provide an insight on the effect of congestion on hydrogen distribution inside the tunnel. No experiments of unignited hydrogen release with vehicles and forced ventilation were performed for these two scenarios. Details about the vehicle size and layout can be found in [4] and [5]. Figure 7 (left) shows the vehicles layout as designed with the pre-process tool.

Figure 7 presents the comparison of the car and train scenario with and without vehicles in terms of maximum concentration, while Figure 8 shows the comparison in terms the flammable volume and volume at near stoichiometric concentration (25-35% v/v). In addition, Table 3 (last row) provides the safety parameters for the train scenario with vehicles inside the tunnel.

For the car scenario the vehicles has no effect on hydrogen dispersion. The cloud is extended few meters from the release point (~6 m) reaching only the first row of the vehicles when it is already diluted. Thus, the effect of vehicles is negligible. However, if the release took place closer to the vehicles, there might be an effect. For the train scenario the vehicles has negligible effect on hydrogen dispersion and the maximum concentration at the deployed sensors. However, there is an effect on the flammable volume, which was reduced in presence of vehicles (by about 12%). This can be justified by the large level of congestion inside the tunnel that confined the flammable mass in smaller volume. If we look at the concentration levels inside the flammable cloud they are slightly higher for the case with vehicles at locations above the vehicles (Figure 8, right).

It is also observed that the maximum flammable volume is achieved few seconds earlier in the case with vehicles compared to the case without and also the flammable cloud exits the tunnel earlier. The volume of the mixture within the range of concentration 25-35 % is practically unaffected.

5.0 CONCLUSIONS

Validation simulations were performed using the ADREA-HF code based on scaled tunnel experiments conducted by HSE with unignited high-pressure hydrogen blowdown releases in presence of forced ventilation. The conditions of the simulated scenarios are representative of a TPRD release from 700 barg in a car and 350 barg in a train. The scaled nozzle size was 2.2 and 4.7 mm for the car and the train, respectively. Two different ventilation rates were considered: 1.25 m/s and 2.4 m/s.

The validation showed a very good agreement for the train scenario with the maximum concentration to be predicted with a relative error lower than 5 % at most of the sensors. The largest under prediction (52 % error) was found at the sensor close to the release at 0.5 m height, but this was due to sensor error. For the car scenario simulation tends to under predict the maximum concentrations at most of the sensors.

In the car scenario, where the release was vertically downwards, the jet impinged the tunnel floor, spread forming a bifurcation and rose up along the tunnel walls (ring-like structure). It accumulated on the ceiling and remained on the top for less than 40 sec. After that time flammable mixture was predicted only on the bottom part of the tunnel around the release. The maximum flammable volume and volume at near stoichiometric concentrations (25-35% v/v) was achieved in less than 10 sec, suggesting that if the ignition has more than 10 sec delay the consequences will be smaller. In the train scenario, the jet was released vertically upwards. It impinged the tunnel ceiling, recirculated, mixed with the ventilation air and spread downwind the release. The flammable cloud was extended along the entire tunnel length downwind the release and exited the tunnel after about 20 sec. The maximum concentration was similar at all sensors indicating that the dilution of the mixture along the tunnel was small. Based on the above remarks, the car scenario can be considered as not very dangerous, while the train scenario is considered dangerous.

A sensitivity study in respect with the ventilation rate was conducted for the train scenario suggesting that the effect of ventilation is high. Even though the flammable cloud was increased with increasing ventilation rate due to the fact that the mixture spreads more along the tunnel, the maximum concentration levels, the volume at near stoichiometric concentrations and the resident time of the flammable cloud inside the tunnel were significantly lower. Another sensitivity study was conducted to investigate the effect of congestion (vehicles inside the tunnel) on dispersion for both the car and train scenario. Congestion showed practically no effect in the car scenario. This was somewhat expected, as the flammable cloud was extended only few meters from the release and the vehicles were placed at a distance of 4 m from the release. For the train scenario, the maximum flammable volume was slightly lower in presence of vehicles, while negligible effect was found on the maximum concentration at the deployed sensors. The cloud formation had similar behavior with the difference that in the case with vehicles the cloud was confined on the top part of the tunnel and between the vehicles (train carriages), and moves faster towards the tunnel opening downwind the release.

To sum up, the results showed good predictive capabilities of the ADREA-HF CFD code. The case with larger release rate and upward release (train scenario) was in better agreement with the experiment. Ventilation rate can be an efficient mitigation measure for tunnels. Congestion inside the tunnel had small effect in the examined scenarios. In the future, simulations of ignited releases based on the HSE tunnel experiments will be performed.

ACKNOWLEDGMENTS

This project has received funding from the Fuel Cells and Hydrogen 2 Joint Undertaking (now Clean Hydrogen Partnership) under Grant Agreement No 826193. This Joint Undertaking receives support from the European Union's Horizon 2020 Research and Innovation program, Hydrogen Europe and Hydrogen Europe Research.

REFERENCES

- [1] Y. Sato, H. Iwabuchi, M. Groethe, E. Merilo and S. Chiba, "Experiments on hydrogen deflagration," *Journal of Power Sources*, vol. 159, no. 144-8, 2006.
- [2] M. Groethe, E. Merilo, J. Colton, S. Chiba, Y. Sato and H. Iwabuchi, "Large-scale hydrogen deflagrations and detonations," *Int J Hydrogen Energy*, vol. 32, p. 2125–33., 2007.
- [3] S. Kudriakov, E. Studer, G. Bernard-Michel, D. Bouix, L. Domergue, D. Forero, H. Gueguen, C. Ledier, P. Manicardi, M. Martin and F. Sauzedde, "Full-scale tunnel experiments: Blast wave and fireball evolution following hydrogen tank rupture," *Int J Hydrogen Energy*, vol. 47, no. 43, pp. 18911-33, 2022.
- [4] S. Mukai, J. Suzuki, H. Mitsuishi, K. Oyakawa and S. Watanabe, "CFD Simulation of Diffusion of Hydrogen Leakage Caused by Fuel Cell Vehicle Accident in Tunnel, Underground Parking Lot and Multi-Story Parking Garage," Washington , 2005.
- [5] A. Venetsanos, D. Baraldi, P. Adams, P. Heggem and H. Wilkening, "CFD modelling of hydrogen release, dispersion and combustion for automotive scenarios," *Journal of Loss Prevention in the Process Industries*, vol. 21, no. 2, pp. 162-184, 2008.
- [6] P. Middha and O. Hansen, "CFD Simulation Study to Investigate the Risk from Hydrogen Vehicles in Tunnels," *Int. J. Hydrogen Energy*, vol. 34, p. 5875–5886, 2009.
- [7] S. Kumar, S. Miles, P. Adams, A. Kotchourko, D. Prichard, H. D., P. Middha, V. Molkov, F. Verbecke, A. Teodorczyk, A. Angebo and M. Zenner, "HyTunnel Final Report, HySafe Deliverable 111," 2009.
- [8] G. Momferatos, S. Giannissi, I. Toliás, A. Venetsanos, A. Vlyssides and N. Markatos, "Vapor cloud explosions in various types of confined environments: CFD analysis and model validation," *Journal of Loss Prevention in the Process Industries*, vol. 75, p. 104681, 2022.
- [9] I. Toliás, A. Venetsanos, N. Markatos and C. Kiranoudis, "CFD modeling of hydrogen deflagration in a tunnel," *Int J Hydrogen Energy*, vol. 39, pp. 20538-4 6, 2014.
- [10] V. Molkov, F. Verbecke and D. Makarov, "LES of hydrogen-air deflagrations in a 78.5-m tunnel," *Combust Sci Technol*, vol. 180, no. 5, pp. 796-808, 2008.
- [11] D. Baraldi, A. Kotchourko, A. Lelyakin, J. Yanez, P. Middha and O. e. a. Hansen, "An inter-comparison exercise on CFD model capabilities to simulate hydrogen deflagrations in a tunnel," *Int J Hydrogen Energy*, vol. 34, no. 18, pp. 7862-72., 2009.
- [12] Y. Sato, H. Iwabuchi, M. Groethe, E. Merilo and S. Chiba, "Experiments on hydrogen deflagration," *Journal of Power Sources*, vol. 159, p. 144–8., 2006.
- [13] W. Houf, G. Evans, E. Merilo, M. Groethe and S. James, "Releases from Hydrogen Fuel-Cell Vehicles in Tunnels," *Int. J. Hydrogen Energy*, vol. 37, p. 715–719, 2012.
- [14] H. Bie and Z. Hao, "Simulation Analysis on the Risk of Hydrogen Releases and Combustion in Subsea Tunnels," *Int. J. Hydrogen Energy*, vol. 42, p. 7617–7624, 2017.
- [15] O. Hansen, E. Hansen, M. Kjellander and R. Martini, "CFD Study to Assess Safety Aspects of TPRD Releases from Heavy-Duty Hydrogen Vehicles and Trains in Tunnels," *Chem. Eng. Trans.*

- , vol. 90, no. , p. 91–96, 2022.
- [16] HyTunnel-D2.3, “Final report on analytical, numerical and experimental studies on hydrogen dispersion in tunnels, including innovative prevention and mitigation strategies,” 2022.
- [17] HyTunnel-D4.4, “Results of the deferred experimental programme and associated activities,” 2022.
- [18] C. LaFleur, G. Bran-Anleu, A. Muna, B. Ehrhart, M. Blaylock and W. Houf, “Hydrogen fuel cell electric vehicle tunnel safety study,” 2017.
- [19] B. Ehrhart, D. Brooks, A. Muna and C. Lafleur, “Risk assessment of hydrogen fuel cell electric vehicles in tunnels,” *Fire Technology*, vol. 56, no. 3, 2019.
- [20] A. Birch, D. Brown and M. S. F. Dodson, “The Structure and Concentration Decay of High Pressure Jets of Natural Gas,” *Combustion Science and Techn.*, vol. 36, no. 5-6, pp. 249-261, 1984.
- [21] I. Tolias, S. Giannissi, A. Venetsanos, J. Keenan, V. Shentsov, D. Makarov, S. Coldrick, A. Kotchourko and K. Ren, “Best practice guidelines in numerical simulations and CFD benchmarking for hydrogen safety applications,” *Int J Hydrogen Energy*, vol. 44, no. 17, pp. 9050-9062, 2019.
- [22] HSE-NCSR, *Private communications with experimentalists confirmed that this sensor is most likely faulty*, 2023.